



Variety of stylolites morphologies and statistical characterization of the amount of heterogeneities in the rock

Alexandre Brouste, François Renard, Jean-Pierre Gratier, Jean Schmittbuhl

► To cite this version:

Alexandre Brouste, François Renard, Jean-Pierre Gratier, Jean Schmittbuhl. Variety of stylolites morphologies and statistical characterization of the amount of heterogeneities in the rock. *Journal of Structural Geology*, 2007, 29, pp.422-434. 10.1016/j.jsg.2006.09.014 . hal-00201784

HAL Id: hal-00201784

<https://hal.science/hal-00201784>

Submitted on 2 Jan 2008

HAL is a multi-disciplinary open access archive for the deposit and dissemination of scientific research documents, whether they are published or not. The documents may come from teaching and research institutions in France or abroad, or from public or private research centers.

L'archive ouverte pluridisciplinaire **HAL**, est destinée au dépôt et à la diffusion de documents scientifiques de niveau recherche, publiés ou non, émanant des établissements d'enseignement et de recherche français ou étrangers, des laboratoires publics ou privés.

1 **Variety of stylolites morphologies and statistical characterization of the**
2 **amount of heterogeneities in the rock**

3

4

5 **Alexandre Brouste**

6 Laboratoire de Modélisation et de Calcul, Université Joseph Fourier, BP 53, 38041 Grenoble, France

7 **François Renard***

8 Laboratoire de Géophysique Interne et Tectonophysique, CNRS, Université Joseph Fourier, BP 53, 38041
9 Grenoble, France & Physics of Geological Processes, University of Oslo, Norway

10 **Jean-Pierre Gratier**

11 Laboratoire de Géophysique Interne et Tectonophysique, Université Joseph Fourier, BP 53, 38041 Grenoble,
12 France

13 **Jean Schmittbuhl**

14 UMR 7516, Institut de Physique du Globe de Strasbourg, 5 rue René Descartes, F-67084 Strasbourg cedex,
15 France

16

17 *Corresponding author:

18 francois.renard@ujf-grenoble.fr, Phone +33 476 82 80 88, Fax; +33 476 82 81 01

Abstract. The surface roughness of several stylolites in limestones was measured using high resolution laser profilometry. The 1D signals obtained were statistically analyzed to determine the scaling behavior and calculate a roughness exponent, also called Hurst exponent. Statistical methods based on the characterization of a single Hurst exponent imply strong assumptions on the mathematical characteristics of the signal: the derivative of the signal (or local increments) should be stationary and have finite variance. The analysis of the measured stylolites show that these properties are not always verified simultaneously. The stylolite profiles show persistence and jumps and several stylolites are not regular, with alternating regular and irregular portions. A new statistical method is proposed here, based on a non-stationary but Gaussian model, to estimate the roughness of the profiles and quantify the heterogeneity of stylolites. This statistical method is based on two parameters: the local roughness (H) which describes the local amplitude of the stylolite, and the amount of irregularities on the signal (μ), which can be linked to the heterogeneities initially present in the rock before the stylolite formed. Using this technique, a classification of the stylolites in two families is proposed: those for which the morphology is homogeneous everywhere and those with alternating regular and irregular portions.

Key words: stylolites, roughness, scaling analysis, heterogeneity

1. Introduction

The geometrical characterization of rough profiles or surfaces is a widespread problem in various geological examples such as erosion patterns (Dunne, 1980; Cerasi et al., 1995), multiphase fluid percolation in porous rocks (Rubio et al., 1989), fractures (Schmittbuhl et al., 1993), or stylolites (Renard et al., 2004). In these studies, the scaling behavior of various data sets was investigated, showing that the statistics at one scale could be extrapolated to another scale using a power law relationship.

For a self-affine function $h(x)$, a scaling relationship is defined when the signal follows a power law relationship under a dilation of a factor λ

$$h(\lambda x) = \lambda^D h(x) \quad (1)$$

where x is the spatial coordinate and h is a scalar field, λ is the scaling scalar, and D is the scaling exponent.

Applying this property to 1D discrete signals, involves working on the increments $\delta h(x)$ of the function h . The self-similar property of a 1D data set $h(x)$ emerges when the increments of the signal follows

$$\delta(h(\lambda x)) = \lambda^H \delta(h(x)) \quad (2)$$

where H is the so-called Hurst exponent (Feder, 1988; Meakin, 1998).

This scaling approach is based on two assumptions on the mathematical properties of the signal. First, increments of the signal have finite variance distribution and, second they are stationary, which means that the statistics are independent of the position along the signal. In the case of a signal with increments that follow a Gaussian distribution (that has a finite variance by definition), the roughness of the signal can be deduced from the scaling exponent.

For a function $h(x)$ with the property:

$$|h(x) - h(y)| \leq C|x - y|^{H_0}, \quad (3)$$

where x and y are two different points along the signal and C is a constant, H_0 is defined as the Hölder exponent (Daubechies, 1992). When the increments of a signal are Gaussian and stationary, the Hölder exponent is equal to the Hurst exponent.

In this contribution, the assumption of Gaussian stationary increments of several 1D data sets is tested, based on roughness measurements of various stylolites in limestones. We show that these profiles do not verify the Gaussian stationary increments property, and we propose a new technique to characterize the statistics of these signals by introducing two parameters: the *localized* roughness exponent H , and a second parameter μ , which characterizes the quantity of irregularities in the system at all scales. Applied to stylolites, this parameter can be used to quantify the degree of heterogeneity in the rock initially present before the stylolitization process. We also show that heterogeneities have an effect only above a millimeter scale.

We first present some examples showing how heterogeneities determine the location of some stylolite peaks. Then the two-parameter statistical description of stylolite roughness is used to help characterize such heterogeneities.

2. The roughness of stylolites

2.1. Self-similar scaling of stylolites

Stylolites are rough surfaces that develop by stress-enhanced dissolution in crustal rocks (Dunnington, 1954; Park and Schot, 1968; Bathurst, 1971; Bayly, 1986). Anticrack models have been proposed to describe their initial stage of nucleation and propagation as a flat interface (Fletcher and Pollard, 1981; Koehn et al., 2003; Katsman and Aharonov, 2006). With time, the stylolites roughen and acquire their typical wavy geometry (Figures 1, 2).

The wide range of morphological geometries of such surfaces makes them difficult to characterize using a simple scaling approach. However, it has been shown that stylolites have self-similar scaling properties (Karcz and Scholz, 2002; Renard et al., 2004; Schmittbuhl et al., 2004). These studies are based on the assumption that the morphological statistics of the stylolites do not vary laterally along the plane of the interface.

Here, the topography of stylolites in limestones was measured using high-resolution laser profilometers that acquire (1+1)D roughness profiles (Figure 2). Some stylolites were split open to reveal the complex 2D geometry of their surface. Using this method, described in Renard et al., (2004), (2+1)D maps of stylolite roughness can be obtained with an accuracy of up to 0.003 mm, on a regular grid of 0.03 to 0.125 mm depending on the kind of profilometer used. The (2+1)D maps were built by combining (1+1)D profiles on a square grid with a constant discretization interval. For each stylolite surface, the result is a (2+1)D height field from which the mean plane was removed by a least-square method.

Using these data, stylolitic 1D profiles were found to show two different self-affine regimes at large and small length scales (Figure 3). Two signal processing techniques were used: the Fourier Power Spectrum (FPS) and the Averaged Wavelet Coefficient (AWC).

FPS decomposition techniques are standard tools used to characterize the scaling behaviour of stationary increments signals (Kahane and Lamarié-Rieusset, 1998). Assuming finite variance stationary increments of a signal, the Hurst exponent H (eq. 2) can be deduced from the power-law behaviour of the Fourier Power Spectrum with

$$FPS(k) \propto k^{-1-2H} \quad (4)$$

where k is the wave number, the inverse of the wavelength (Barabási and Stanley, 1995).

Wavelet series (or wavelet decompositions) constitute a powerful tool for processing signals in which different scales are combined (Meyer and Roques, 1993). Various signals can be reconstructed knowing the coefficients of their wavelet decomposition, and for

compactly supported wavelets (Daubechies, 1992) any 1D profile, $h(x)$, can be decomposed into a wavelet series having the following summation:

$$h(x) = \sum_{j=0}^{+\infty} \sum_{i=0}^{2^j-1} c_{i,j} \psi(2^j x - i) \quad (5)$$

where $c_{j,i}$ are the wavelet coefficients indexed by (j,i) and ψ is the so-called mother wavelet (generating all the wavelets by expansion of a factor 2^j and by a translation i).

Using this method, the self-similar behaviour of a signal emerges as the average wavelet coefficient AWC satisfies:

$$AWC(l) \propto l^{H+0.5}, \quad (6)$$

where l is the spatial wavelength (Simonsen *et al.*, 1998).

These two techniques provide a scaling relationship and the Hurst exponent is directly related to the slope of the spectra. In the case of a signal with Gaussian and stationary increments, the Hölder exponent is equal to the Hurst exponent.

In stylolites, these two signal processing techniques give the same Hurst exponent (eq. 2), $H = 0.5$ for the large length scales and $H = 1.1$ for small length scales (Figure 3, see also Renard *et al.*, 2004).

The measurements also show that a sharp cross-over length scale close to the millimeter scale separates the two regimes. This characteristic length scale has been interpreted as a crossover length emerging from the competition between two forces: surface tension dominates at small wavelengths, whereas elastic interactions dominate at large wavelengths (Renard *et al.*, 2004; Schmittbuhl *et al.*, 2004).

Using the same data sets, it can also be shown that a stylolite can be wavy at one point and rather flat at another point (Figure 2), suggesting that the statistical properties vary along the profiles. Therefore, the Gaussian stationary increments hypothesis must be called into

question. This spatial variation in statistical properties along a single stylolite is not accounted for in current models of stylolite roughening.

2.2. *Heterogeneities along stylolites*

Various examples both from nature and experiments show that heterogeneities in rocks help either to localize dissolution pits or to deflect the dissolution surface along a single stylolite at all scales. [Figure 4a](#) shows experimental microstylolites along quartz grains ([Gratier et al., 2005](#)). Dissolution pits ([Figure 4b](#)) are systematically located at the bottom of each conical-shaped stylolite structure. Due to the fit of the two opposite grain surfaces, the pits of the lower grain stylolite surface are located just in front of the stylolitic peak of the upper grain and vice versa. The explanation is that pits develop at intersections of crystal dislocations with the grain surface and determine the stylolite peak location.

[Figure 4c](#) shows the indenting of a mineral (quartz) by another mineral (mica). In this case, the mica grains along the dissolution surface are responsible for the local dissolution peaks. Mica distribution determines the location of the peaks location.

The same geometry may be observed along columnar stylolites in limestones ([Figure 4d](#)). However, the interpretation is different as the two parts of the rock have the same composition. In this case, the geometry of the columnar stylolite is probably determined by preexisting micro-fractures as is clearly the case in the example shown in [Figure 4e](#) where a fracture controls the shape of the peak. Finally, [Figure 4f](#) shows several dissolution seams that are deflected by hard objects: pyrite (black) or quartz pressure shadows (white). In this case, the hard objects located in the dissolution plane deflect it, thereby contributing to roughening of the dissolution surface.

All these examples show that the location of some stylolite peaks is not purely random but rather partially controlled by the distribution of heterogeneities. The statistical properties of stylolites should depend on the distribution of these heterogeneities, and therefore vary in

space along a single stylolite. It would appear relevant to integrate the presence of non-uniformly distributed heterogeneities at all scales in the modeling of stylolites and test their potential effect on the final geometry.

3. A two-parameter statistical description of the roughness of 1D stylolite profiles

The wide range of morphologies of stylolites (Figure 1) and the alternating smooth and irregular portions of the same stylolite (Figures 2, 5a), suggests that the Gaussian stationary increments assumption should be tested. In this section we show that it is not possible to obtain all stylolite morphologies from a single parameter scaling relationship (e. g. a Hurst exponent).

Figure 5b represents the increments of a 1D stylolite. These increments are calculated as the height difference between two successive points, and therefore represent a first order derivative of the original signal of Figure 5a. In this incremental signal, the existence of many large jumps and long tails in the histogram (Figure 5c) differentiate the signal from a synthetic fractional Gaussian noise signal (Figure 5h). Therefore, the Gaussian self-similar stationary increments property can be excluded for stylolite signals and a simple scaling relationship using a single Hurst exponent is not sufficient to explain the measured signals. The following section proposes a new technique that can accommodate the large jumps of Figure 5b so that it can be applied to stylolites. This analysis has been tested on all the available stylolites surfaces, and show similar properties.

3.1. The Simple Branching Process Wavelet Series method

Mathematicians commonly use two different techniques to deal with the large jumps similar to those shown in Figure 5b. The first technique is to select a non-Gaussian self-similar stationary increment model with infinite variance, also called stable Lévy motion

(Samorodnitsky and Taqqu, 1994). Stable Lévy motions contain two parameters: the frequency of the jumps and the average size of these jumps. Applied to stylolites, microfractures densities in the rocks can be associated with the frequency of jumps for instance and estimated by specific methods. However, in such models, the roughness cannot be identified from the scaling relationship because the roughness and the scaling exponents are not similar. The Lévy models are avoided in the following discussion. The second technique is a non-stationary Gaussian model with scaling properties, where the roughness can be estimated. According to Samorodnitsky and Taqqu (1994), neither of these techniques is superior to the other.. In the following section, the non-stationary Gaussian model is used and referred to as the Simple Branching Process Wavelet Series (in short SBPWS).

3.2. Construction of SBPWS profiles in one dimension

Simple Branching Processes (also called Galton-Watson processes, see Harris, 1969) are stochastic trees built by an incremental branching process at all scales. In the case of Simple Branching Process Wavelet Series (SBPWS), each node of the tree has the same probability of having either one or two branches (see Figure 6a). In the following, $1 < \mu < 2$ corresponds to the average number of sons at each node. For a node of the tree, $(2 - \mu)$ represents the probability of having only one branch.

SBPWS models are particular random *lacunary* wavelet series (Jaffard, 2000) based on simple branching processes. Lacunary refers to the property that only a small number of coefficients in the series are non-vanishing, more precisely those indexed by an elementary branching process and corresponding to the branches of Figure 6a. SBPWS is defined by:

$$SBPWS(x) = \sum_{j=0}^{\infty} 2^{-jH} \sum_{i \in \Lambda(\mu)} \varepsilon_{j,i} \psi(2^j x - i) \quad (7)$$

where x is the spatial coordinate, H is the fractional parameter, $\Lambda(\mu)$ is the elementary branching process of parameter μ , $\varepsilon_{j,i}$ are a family of independent Gaussian standard random variables and ψ is a wavelet-like function.

Only wavelets with coefficients indexed by the stochastic sub-tree Λ (of non-vanishing coefficients) contribute to the roughening of the initial flat profile (see [Figure 6b](#)). Therefore, the stochastic tree process Λ locally deforms the 1D profile, at all the tree branches.

In this model, elementary forms of the deformation are given by the shape of the mother-function ψ . A difficulty with modeling a stylolitic structure is to choose the function ψ , which corresponds to the shape of each dissolution increment. However, it has been shown that the statistics of a simulated signal do not depend on the shape of ψ , as long as this function has the same property as an individual wavelet ([Brouste, 2006](#)).

In nature, the stylolite shape varies from columnar to conical ([Figures 1, 4](#)) and these two kinds of shape might be related to the shape of microscopic increment of dissolution: either rectangular for columnar stylolites, or triangular for the conical ones. As a consequence, a choice must be made in the mathematical modeling between rectangular or triangular increments or a specific parameter used that may express all the intermediary shapes. Moreover, columnar stylolites are rather specific, being associated either with microfractures ([Figure 4d and 4e](#)) or with non-consolidated material ([Gratier et al., 2005](#)). In order to avoid the use of a third parameter, the shape of the function ψ , which might hide the effect of the two other parameters, a triangular function was chosen for ψ ([Figure 6b, inset](#)). Note that the choice of the shape of this function ψ does not modify the statistical properties of the synthetic signal.

The natural stylolites that were examined in this study can be modeled with such an elementary triangular shape. By varying the parameters H and μ , one can generate synthetic profiles that have stylolite-like patterns (Figure 7; Appendix A gives the algorithm to build these synthetic stylolites). These synthetic profiles, unlike those generated by previous models, exhibit two important properties of the natural stylolites:

- i) the variability of the roughness between independent stylolite profiles;
- ii) the variability of the roughness within a single profile, with alternating regular and irregular portions.

3.3. Parameters H and μ

The parameters H and μ have distinct visual effects on the synthetic profiles. The irregularities on the whole profile are quantified by the parameter μ : for instance, at the n^{th} order branches, there are, on average, μ^n non-vanishing coefficients and then μ^n branches of the tree, corresponding to μ^n stages of deformation of the initially flat profile. When μ is close to 2, there are irregularities everywhere along the profile. When μ decreases to 1, there are alternating irregular and regular portions along the profile. Finally, when μ is equal to 1, there are no more irregularities along the signal.

The amplitude of the deformation (only where it is deformed) depends on the scale, on a random Gaussian variable, and on a fractional exponent H that can be considered to be a local roughness parameter. In this sense, H is indicative of the nature of the irregularity and the amplitude of the profile variations. When H tends to 0 the profile is irregular and looks “noisy”. This property is also called antipersistence: locally a valley in the signal has a greater probability of being followed by a hill. When H is close to 1, the profile roughness is smoother and a valley or a hill in the signal tends to extend locally. This property is called persistence (Meakin, 1998).

3.4. Measurements of H and μ on a 1D data set

As stated previously, the SBPWS have scaling properties that no longer involve a unique stationary Hurst exponent. SBPWS provides self-affine behavior either in the 1D Average Wavelet Coefficient technique or in the Fourier Power Spectrum, and is defined by a power-law in both scale and frequency domains, respectively (Brouste, 2006):

$$AWC(l) \propto l^{1 - \log_2 \mu / 2 + H} \quad (8)$$

and

$$FPS(k) \propto k^{-2 + \log_2 \mu - 2H} \quad (9)$$

where H and μ are the two parameters of the SBPWS method. When $\mu = 2$, equations (8) and (9) are reduced to the Gaussian stationary case described in equations (4) and (6).

Note that in the SBPWS method, the values of H and μ cannot be determined by a simple regression to the 1D Fourier and AWC spectra, as done previously by Renard et al. (2004), because the following system of equations, whose determinant is equal to zero, is underdetermined:

$$\begin{cases} 2H - 2 + \log_2 \mu = a \\ H - 1 + \log_2 \mu / 2 = b \end{cases} \quad (10)$$

Here a and b are the slopes measured by linear regression on the FPS spectrum and on the AWC spectrum, respectively.

Therefore, a more complex tool must be used, such as the s-generalized variations method (Istas and Lang, 1997) to obtain estimated values of H and μ at large and small length scales. This method, detailed in Appendix B, was applied to estimate H and μ in the stylolites that were measured (Table 1).

4. Application to natural stylolites

4.1. Parameters H and μ for the stylolites

To estimate the parameters μ and H , from both sides of the cross-over length scale, it is necessary to observe how the estimators of Appendix B behave when the length scale decreases (as n increases), from large scales to small scales through the cross-over length scale (Figure 8a-b). Large length scales values are taken at the cross-over length scale and small ones are taken at the discretization scale in order to use the greatest number of points in the two different patterns.

The results presented in Table 1 are based on averaged estimations of a series of 256 to 512 parallel stylolite profiles, each profile being regularly discretized on 512 to 1024 points. This gives the large length scale and the small length scale parameters H and μ for all the stylolites that have been measured.

4.2. Geometrical characterization

Most of the information on μ and H variability belongs to the large length scale parameters (see Table 1). In fact, small length scale parameters have almost similar values (μ from 1.2 to 1.4 and H from 0.6 to 0.85) for all samples except S12A and S13A. These results are also found on experimental microstylolites in quartz (Sdiss1 and Sdiss2 in Table 1, Gratier et al., 2005), suggesting that an physical process smoothes the stylolites at small wavelengths.

Plotting the results of the analysis in μ versus H space, one can distinguish between two classes of stylolites at long wavelengths. (Figure 10). A first class, called homogeneous stylolites, contains two kinds of profile: i) the almost-everywhere irregular stylolites (Sjura1 or S12A) and ii) the smooth stylolites (S11C or S10A). For both kinds, the parameter μ is close to 2 (greater than 1.75), which represents few heterogeneities in the rock. Irregular stylolites have a localized roughness parameter H that varies around 0.5 (0.4 to 0.5 in the results obtained here), contrary to smooth stylolites where H is close to 1. Stylolites of this class can be simulated by dynamic surface growth models such as the

Langevin growth equations (Renard et al., 2004; Schmittbuhl et al., 2004) because profiles have the same kind of irregularity almost everywhere.

The second class of stylolites, called heterogeneous stylolites, contains a variety of morphologies. In this case the parameter μ is close to 1.5 (stylolites S3b or S0_8). These stylolites are non-stationary. In this case, the initial heterogeneities in the rock that are reached by the stylolite during its propagation are recorded in the stylolitic signal. More exactly, above the millimeter scale, where elastic interactions dominate, heterogeneity may be seen in the signal. Below the millimeter scale, where surface tension dominates, this heterogeneity has disappeared.

Agglomerative nesting, clustering methods and principal component analysis (not shown here) have been performed and indeed show that statistical analysis supports the classification of stylolite morphologies in two different classes.

4.3. Simulations

Given a set of parameters (H , μ) for both regimes (large and small length scale behaviors from both parts of the cross-over length scale), the behavior of all measured stylolites can be reproduced with two SBPWS. This technique can be used to simulate a wide range of stylolite morphologies (Figures 7, 9):

- those which are close to stationary profiles (μ close to 2);
- smooth profiles with H close to 1 to irregular profiles with a fractional exponent H ;
- more heterogeneous profiles with alternating smooth and irregular zones (where $\mu \neq 2$).

An interesting perspective would be to use the shape and regularity of stylolites in order to evaluate the heterogeneity of the rock before or during the stylolitic process, and therefore better characterize under which conditions (depth, cohesion of the sediment) stylolites form. Another perspective would be to choose a different noise (a fractional stable noise for

instance) in the Langevin growth equations proposed in Renard *et al.* (2004) and Schmittbuhl *et al.* (2004). This remains a real prospect for continuous stylolites models and, more generally, a theoretical extension of rough surface growth models.

4. Conclusion

When the increments of a mathematical function are not stationary (in other words their statistics vary along the coordinate), or the variance of their distribution is infinite, standard tools (Fourier spectrum or average wavelet coefficient analysis) fail to capture a roughness property from a scaling property.

Therefore, an extension of such tools to non stationary signals is proposed here by using a two-parameter approach. One of the parameters, the local roughness exponent H , describes the noisiness or waviness of the signal. The second parameter, μ , describes how the statistical properties vary along the signal.

Applied to stylolites, two kinds of geometry can be distinguished.

i) Stationary stylolites, where the statistics do not vary along the stylolite. For this kind of stylolite, two sub-families can be defined: stylolites that are almost flat everywhere and those that are very wavy everywhere.

ii) Non-stationary stylolites where wavy portions alternate with flatter ones. In this case, we propose that heterogeneities initially present in the rock strongly control the stylolite morphology. To our knowledge, this second kind of stylolite, which has fossilized the heterogeneities of the rock in its morphology, has not been previously quantified. Detailed microstructural and chemical mapping studies focusing on the characterization of heterogeneities around stylolites would surely bring new information.

This difference between the two families of stylolites is detected only for wavelengths greater than a crossover scale close to the millimeter. Below this scale, the statistics of all

346 the stylolites are very homogeneous, indicating that a physical process, probably driven by
347 the minimization of the local curvature, smoothes the stylolites at small scales.

348

349 **Acknowledgments**

350 This project was supported by the CNRS (ATI and DyETI programs).

351

352 **Appendix A: Algorithm to build synthetic signals**

```

353 %////////// Run the styloprocess function //////////
354 %Matlab© program to create the stylolites of Figure 7
355 %Parameters of the simulation
356 %K: depth of the tree (2^K+1 is the number of points on the
357 profile)
358 %mu: heterogeneity parameter (between 1 and 2)
359 %H: local roughness exponent (between 0 and 1)
360
361 function (stylolite) = styloprocess (K,mu,H)
362
363 x=linspace(0,2,2^(K-1));
364 y=1-abs(x-1);
365 psi=(-y,y,0);
366 trees=createtree(K,(2-mu));
367 profile=reconstruct(K,trees,H,psi);
368 plot(surface);
369
370 %////////// Galton-Watson Tree //////////
371 function (trees)=createtree(K,p)
372
373 randn('state',sum(100*clock));
374 trees(1)=randn(1);
375 for m=0:K-1
376     for l=0:2^m-1
377         zfather=2^m+l;
378         zson1=2*zfather;
379         zson2=2*zfather+1;
380         if (trees(zfather)==0)
381             trees(zson1)=0;
382             trees(zson2)=0;
383         else
384             if (rand(1)<p)
385                 if (rand(1)<1/2)
386                     trees(zson1)=randn(1);
387                     trees(zson2)=0;
388                 else
389                     trees(zson2)=randn(1);
390                     trees(zson1)=0;
391                 end
392             else
393                 trees(zson1)=randn(1);
394                 trees(zson2)=randn(1);
395             end
396         end
397     end
398 end
399

```

```

400 %///////////////// Reconstruction ///////////////////
401 function (sig)=reconstruct(K,trees,H,psi)
402
403 sig=zeros((1, 2^K+1));
404 for m=0:K
405     psim=();
406     for j=1:2^(K-m)+1
407         psim(j)=2^(m/2)*psi(2^(m)*(j-1)+1);
408     end
409     sigtemp=(0);
410     for l=0:2^m-1;
411         zfather=2^m+l;
412         psitemp=2^(-m*(H+1/2))*trees(zfather)*psim;
413         sigtemp=(sigtemp,psitemp(2:2^(K-m)+1));
414     end
415     sig=sig+sigtemp;
416 end

```

417 **Appendix B: Calculation of H and μ on 1D signals**

418 A 1-D profile $h(x)$ is observed on a regular grid (at space $x_i = i / 2^n$ for $i = 0 \dots 2^n - 3$).

419 Note the second order variation, an approximation of the second order derivative, at
420 point x_i , by

$$421 \quad \Delta_a h\left(\frac{i}{2^n}\right) = \sum_{l=0}^2 a_l h\left(\frac{i+l}{2^n}\right) \quad (\text{B1})$$

422 where $a = (a_0, a_1, a_2) = (-1, 2, -1)$.

423 Summing the $2^n - 3$ variations $\Delta_a h(i / 2^n)$ for $i = 0 \dots 2^n - 3$, the statistic $V_{n,s}$ is obtained:

$$424 \quad V_{n,s} = \sum_{i=0}^{2^n-3} \left(\Delta_a h\left(\frac{i}{2^n}\right) \right)^s \quad (\text{B2})$$

425 where $s = 2$ (also called quadratic variations) or $s = 4$ (quadric variations). This statistics

426 behave according to a power law depending on the parameters H and μ , with

$$427 \quad V_{n,s} \approx 2^{n(sH - \log_2 \mu)}.$$

428 If we note,

429
$$W_{n,s} = \log_2 \left(\frac{V_{n-1,s}}{V_{n,s}} \right) \quad (\text{B3})$$

430 then $W_{n,s} \xrightarrow{n \rightarrow \infty} sH - \log_2 \mu$ and by linear combination, either μ or H is obtained. The

431 estimators are respectively:

432
$$\mu_n = 2^{2W_{n,2} - W_{n,4}} \text{ and } H_n = \frac{1}{2}(W_{n,4} - W_{n,2}). \quad (\text{B4})$$

433

434 **References**

- 435 Barabási, A. L. and Stanley, E. H., 1995. Fractal concepts in surface growth. Cambridge
436 University Press. New York.
- 437 Bathurst, R. 1971. Carbonate sediments and their diagenesis. Elsevier Science, New York.
- 438 Bayly, B. 1986. Mechanisms for development of stylolites. *Journal of Geology* 94, 431-
439 435.
- 440 Brouste, A. 2006. Simple Branching Process Wavelet Series, submitted to *Journal of*
441 *Theoretical Probability*.
- 442 Cerasi, P, Mills, P., and Fautrat, S., 1995. Erosion instability in a non consolidated porous
443 medium. *Europhysics Letters* 29, 215-220.
- 444 Daubechies, I., 1992. Ten Lectures on Wavelets. Society for Industrial and Applied
445 Mathematics, Philadelphia.
- 446 Dunne, T., 1980. Formation and controls of channel networks. *Progress in Physical*
447 *Geography* 4, 211-239.
- 448 Dunnington, H., 1954. Stylolites development post-date rock induration. *Journal of*
449 *Sedimentary Petrology* 24, 27-49.
- 450 Feder, J., 1988. Fractals. Plenum Press.
- 451 Fletcher, R. A., and Pollard, D. D., 1981. Anticrack model for pressure solution surfaces.
452 *Geology* 9, 419-424.
- 453 Gratier, J., Muquet, L., Hassani, R. and Renard, F., 2005. Experimental microsylolites in
454 quartz and modeled application to natural stylolitic structures. *Journal of Structural*
455 *Geology* 27, 89-100.
- 456 Harris, T.E., 1963. The Theory of Branching Processes. Springer-Verlag, Berlin.

- 457 Istas, J., and Lang, G., 1997. Quadratic variations and estimation of the local Hölder index
458 of a Gaussian process. *Annales Institut Henri Poincaré* 33(4), 407-436.
- 459 Jaffard, S., 2000. On Lacunary Wavelet Series. *Annales Institut Henri Poincaré* 10, 313-
460 329.
- 461 Kahane, J. P., and Lemarié-Rieusset, P. G., 1998. *Séries de Fourier et ondelettes*. Editions
462 Cassini, Paris.
- 463 Karcz, Z., and Scholz, C. H., 2003. The fractal geometry of some stylolites from the
464 Calcare Massiccio Formation, Italy. *Journal of Structural Geology* 25, 1301-1316.
- 465 Katsman, R., Aharonov, E., and Scher, H., 2006. A numerical study on localized volume
466 reduction in elastic media: some insights on the mechanics of anticracks. *Journal of*
467 *Geophysical Research* 111, B03204. doi:10.1029/2004JB003607.
- 468 Koehn, D., Arnold, J., Malthe-Sorrensen, A., and Jamtveit, B., 2003. Instabilities in stress
469 corrosion and the transition to brittle failure. *American Journal of Science* 303, 956-971.
- 470 Meakin, P., 1998. *Fractals: scaling and growth far from equilibrium*. Cambridge University
471 Press, New York.
- 472 Meyer, Y., and Roques, S., 1993. Progress in wavelets analysis and applications. In:
473 *Proceedings of the International Conference “Wavelets and Applications”*, Editions
474 Frontières.
- 475 Park, W. and Schot, E., 1968. Stylolites: their nature and origin. *Journal of Sedimentary*
476 *Petrology* 38, 175-191.
- 477 Samorodnitsky, G. and Taqqu, M. S., 1994. *Stable Non-Gaussian Random Processes:*
478 *Stochastic models with infinite variance*. Chapman and Hall, New-York.
- 479 Schmittbuhl, J., Gentier, S., and Roux, S., 1993. Field measurements of the roughness of
480 fault surfaces. *Geophysical Research Letters* 20, 639-641.

- 481 Schmittbuhl, J., Renard, F., Gratier, J.-P., Toussaint, R., 2004. The roughness of stylolites:
482 Implications of 3D high resolution topography measurements. *Physical Review Letters* 93,
483 238501.
- 484 Simonsen, I., Hansen, A., and Nes, O.M., 1998. Using wavelet transforms for Hurst
485 exponent determination. *Physical Review E* 58, 2779-2787.
- 486 Renard, F., Schmittbuhl, J., Gratier, J.-P., Meakin, P., and Merino, E., 2004. Three-
487 dimensional roughness of stylolites in limestones. *Journal of Geophysical Research* 109,
488 B03209. doi:10.1029/2003JB002555.
- 489 Rubio, M. A., Edwards, C. A., Dougherty, A., and Gollub, J. P., 1989. Self-affine fractal
490 interface from immiscible displacement in porous media. *Physical Review Letters* 63,
491 1685-1688.
- 492

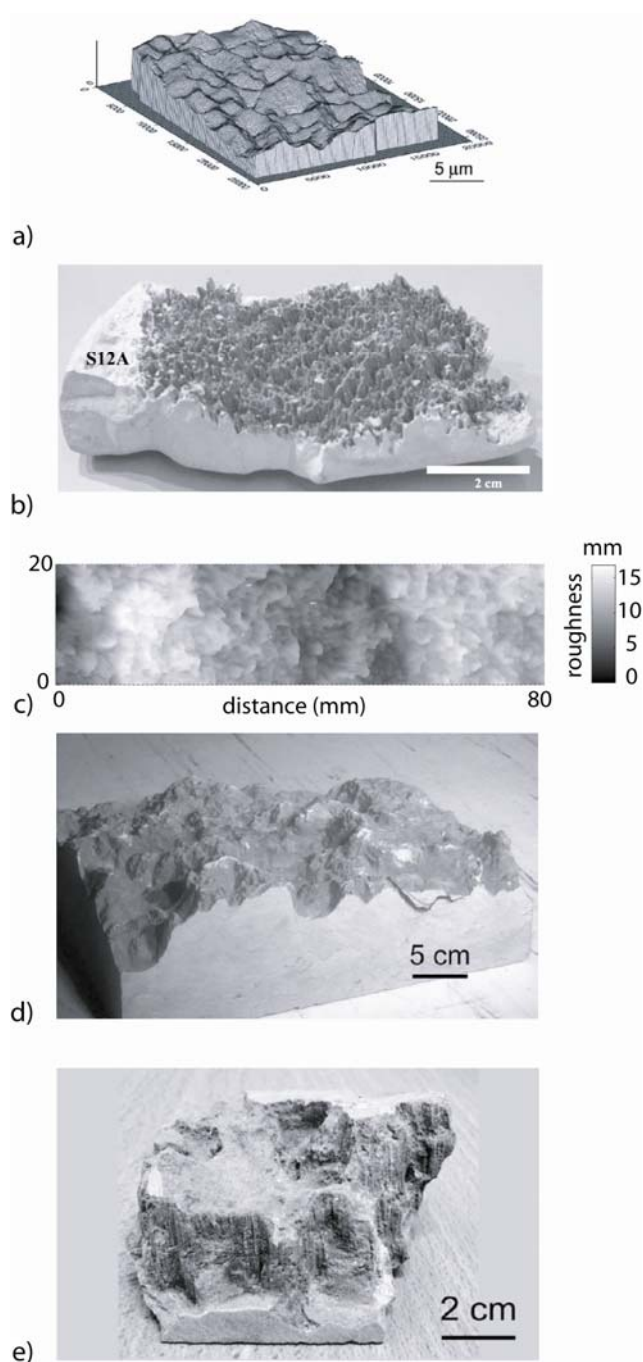
493 **Figures & Table**

Figure 1. Various shapes of stylolites. a) Digital elevation model of a microstylolites measured at the contact between experimentally deformed quartz grains (after Gratier et al., 2005, isotropic scale). b) 2D stylolite surface S12A in a limestone. c) Roughness field of the surface S12A measured using a laser profilometer (Renard et al., 2004). d) Stylolite S3b showing local variations in roughness, with alternating smooth and rougher areas. Such lateral roughness variations are a good visual indicator that the roughness statistics are not the same all along the profiles. e) Stylolite in limestone with vertical peaks showing strong lateral variations in height. It was not possible to measure the roughness of such stylolites because of local overhangs.

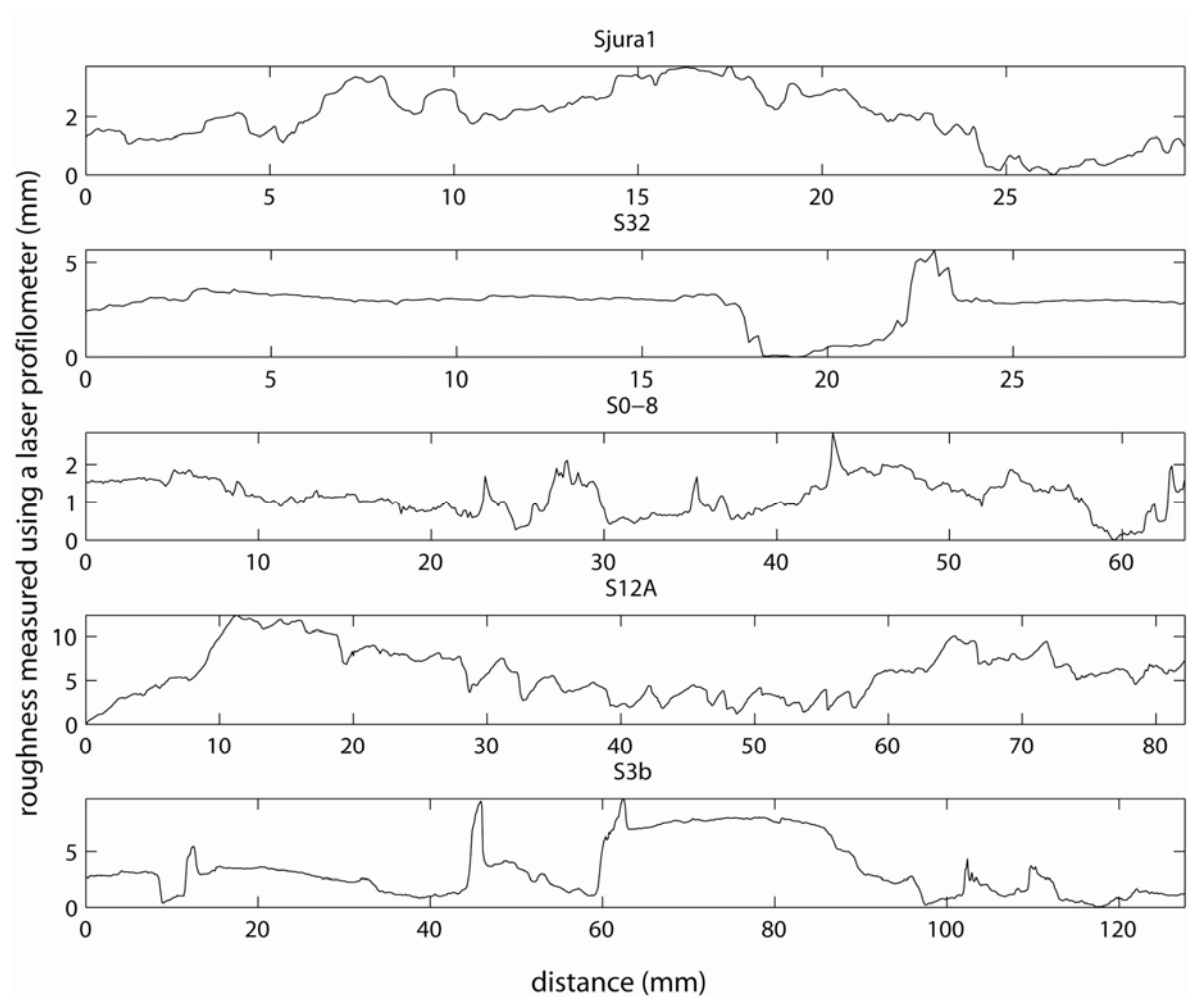


Figure 2. Examples of the 1D roughness of different stylolites in limestones measured using laser profilometer (see Renard et al. (2004) for the measurement technique). The waviness of the stylolite, characterized by the Hurst exponent H varies from sample to sample. Moreover, within the same stylolite, regions with smooth or wavy roughness can be defined, and characterized by the amount of irregularities defined by the parameter μ (see text). Scales are given in mm. The characteristics of each profile are given in Table 1.

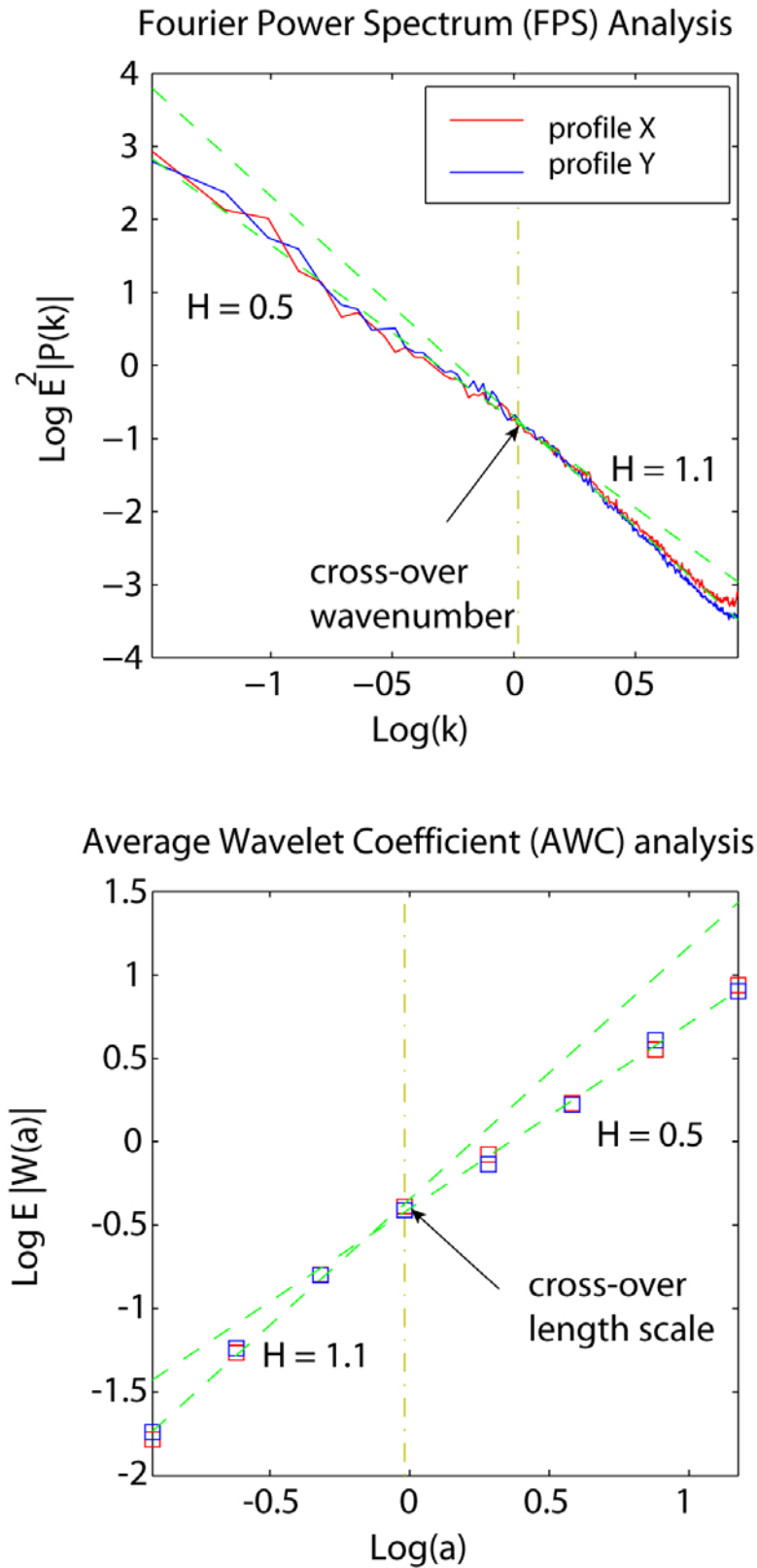


Figure 3. FPS (top) and AWC (bottom) for the stylolite Sjura1. These two independent scaling methods show that there is a crossover at $\sim 1\text{mm}$ between the small wavelengths ($H \sim 1.1$) and the large wavelengths ($H \sim 1.5$).

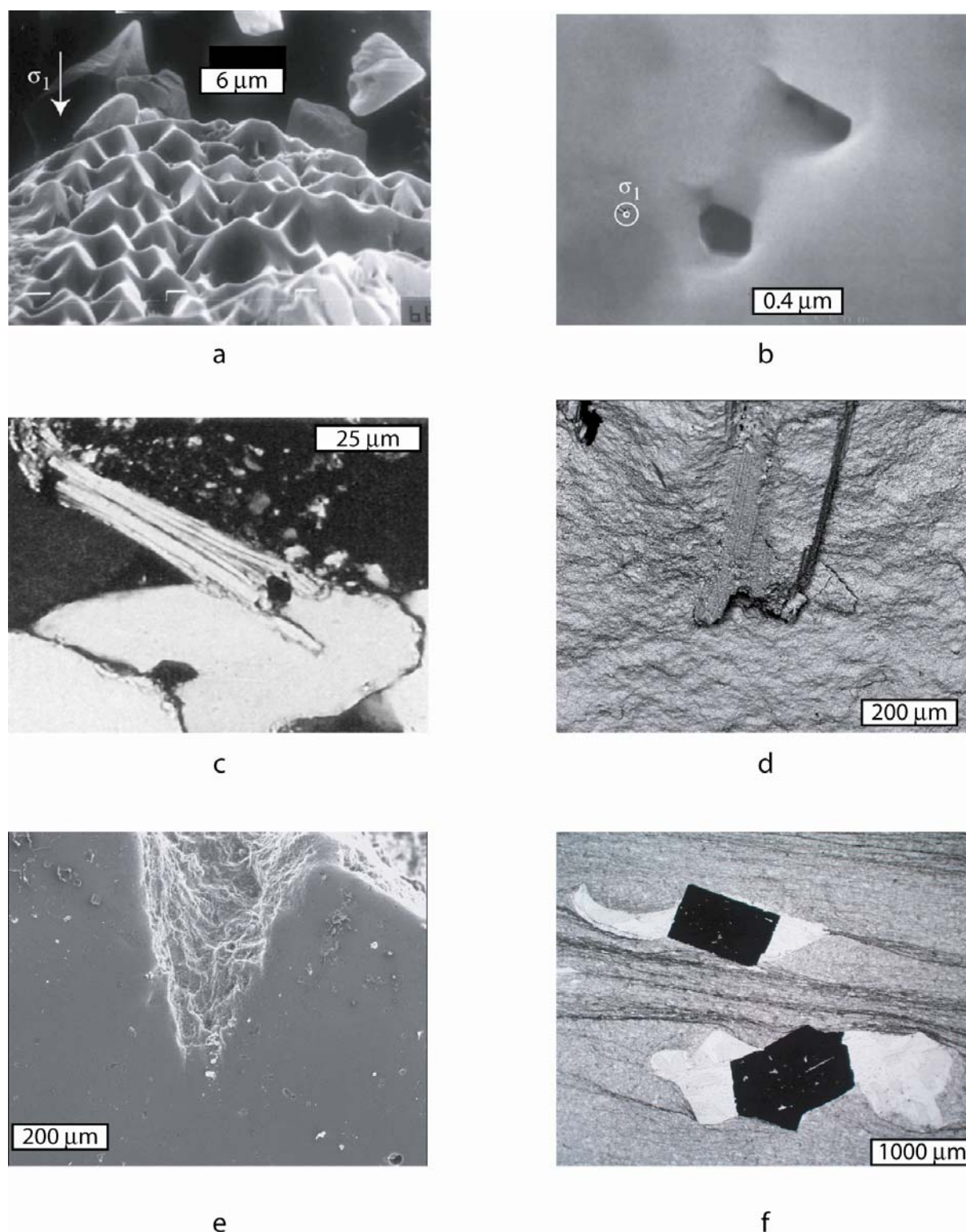


Figure 4. Heterogeneities associated with stylolites. a-b) Microstylolite on a quartz grain (Gratier et al., 2005) and zoom on two dislocation pits where deformation is localized. c) Mica indenting a quartz grain in a North Sea Sandstone and showing a wavy interface at the grain scale. d-e) Zoom on stylolite peaks in the sample Sjura1. f) Dissolution seams (“flat” stylolites) deflected by pyrite crystals and quartz pressure shadows in a metamorphic schist from Bourg d’Oisans (Alps, France).

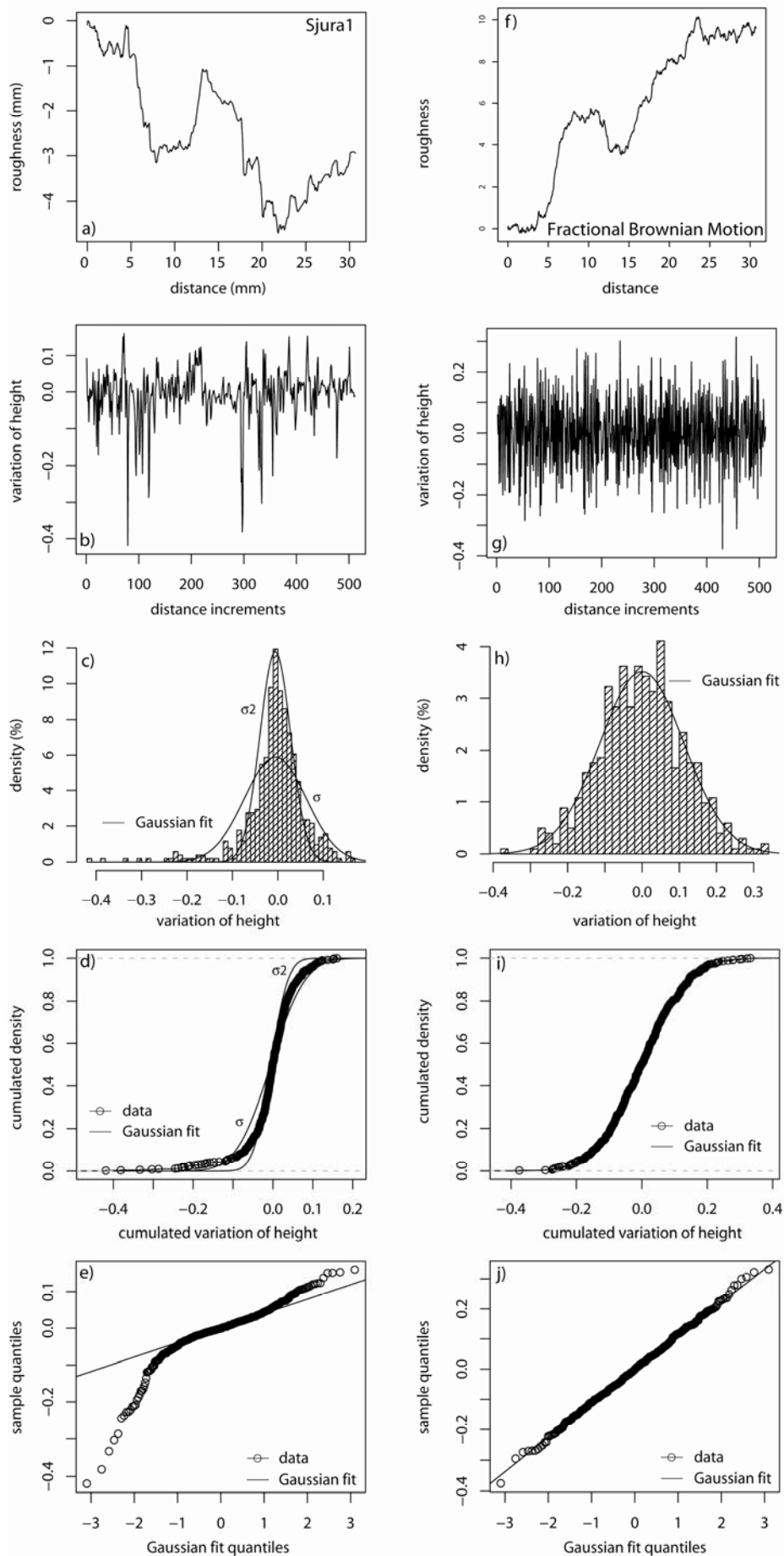


Figure 5. a) Laser roughness measurement of a 1D profile from the stylolite Sjura1. b) Local increments of the stylolite Sjura1, corresponding to the first order discrete derivative of profile a). c) Histogram of the increments of b) with the best Gaussian fits represented by the two curves, which have the same standard deviation (σ) and half the standard deviation ($\sigma/2$) of the stylolite data. d) Cumulative distribution function of b). The two lines represent the best Gaussian fits as in b). The large jumps of the local increments and the long tails in the histogram cannot be accounted for using Gaussian stationary statistics (plain curves). e) Quantile-quantile plot that adjusts the sample distribution in d) against the best Gaussian distribution. This corresponds to the difference between the data and the Gaussian estimate of d). For a Gaussian distribution a straight line should be observed. f -j) Same plots for a synthetic fractional Brownian motion. In the quantile-quantile plot, the synthetic signal and the Gaussian best fit adjust perfectly on a straight line, showing that the fractional Brownian motion is a Gaussian stationary increments signal.

539

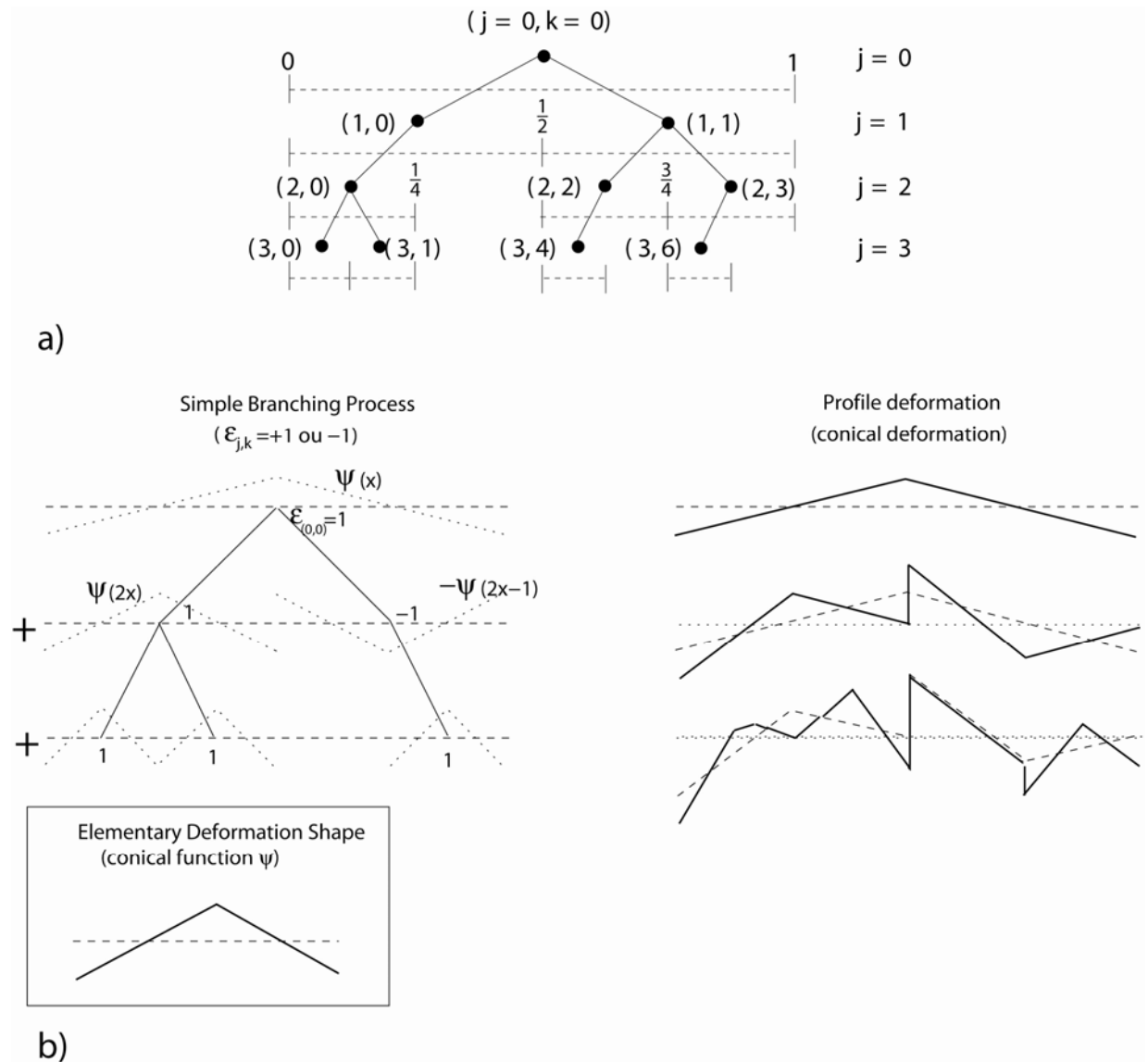


Figure 6. a) Galton-Watson tree (simple branching process) and indexes for the wavelet construction. b) Construction of a synthetic 1D profile using the branching process wavelet series. Such technique is used to build the synthetic signals of Figure 7, using the algorithm given in Appendix A.

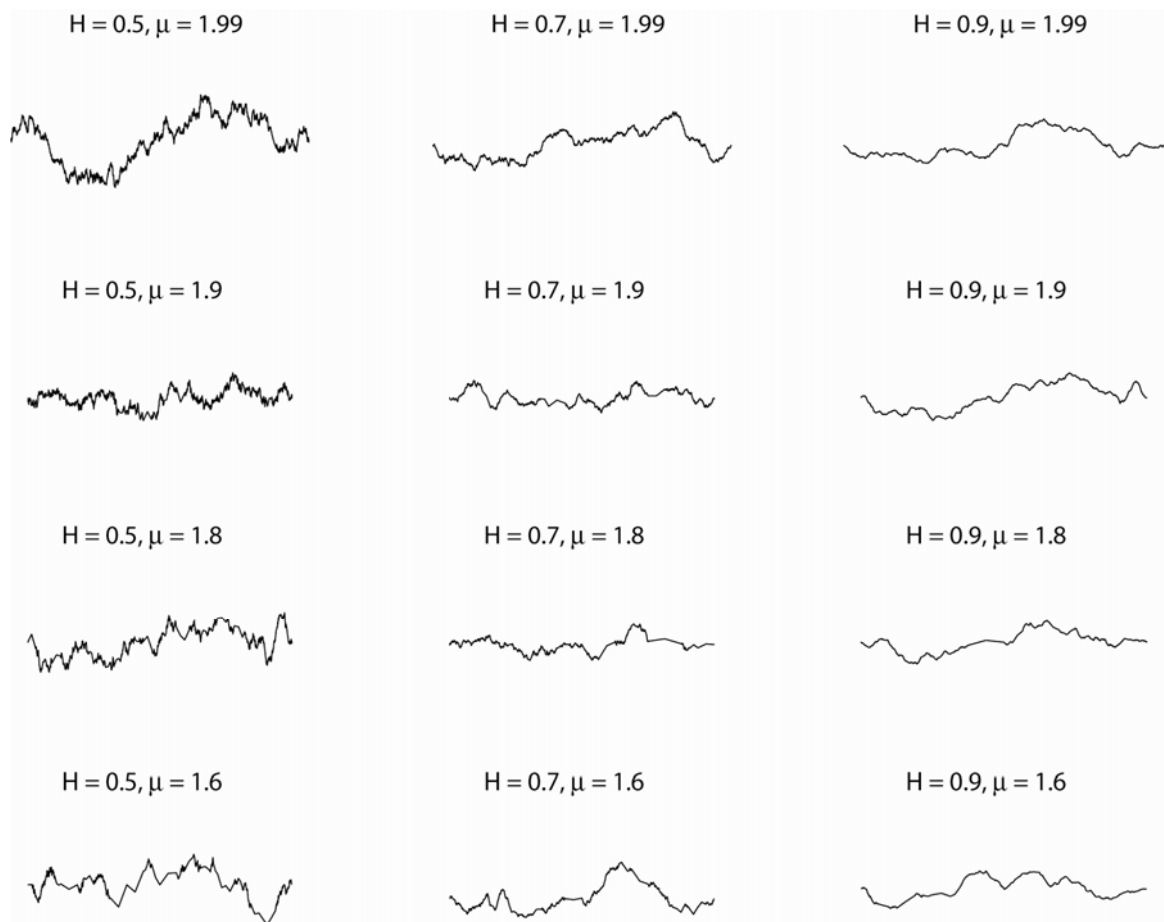


Figure 7. Simulated stylolites with statistical roughness properties characterized by two parameters. The variability in the stylolite morphology is controlled by H which describes the apparent noisiness (smoothness) of the roughness, and μ which describes the spatial variability (heterogeneities at all scales) along the stylolite.

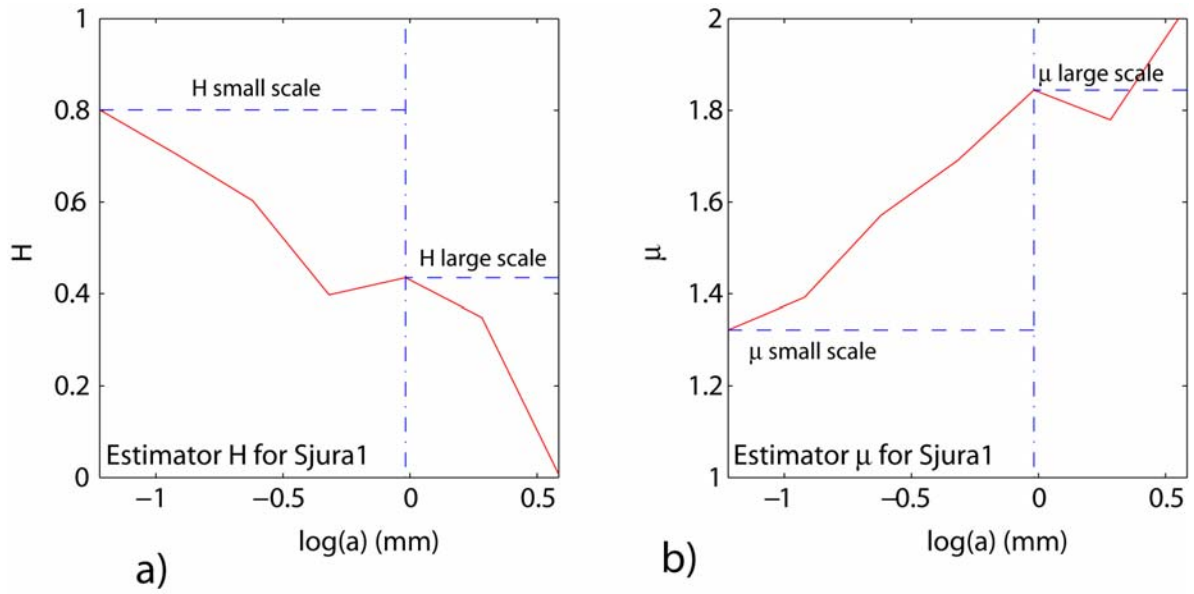


Figure 8. a, b) Estimators of μ and H for the stylolite Sjura1 at small length scales and large length scale. As the length-scale a decreases (n increases in the equations of Appendix B, where n represents the level of branching in Figure 6), the estimated values converge respectively to H and μ just above the cross-over length scale for large length scales and as allowed by the precision for small length scales.

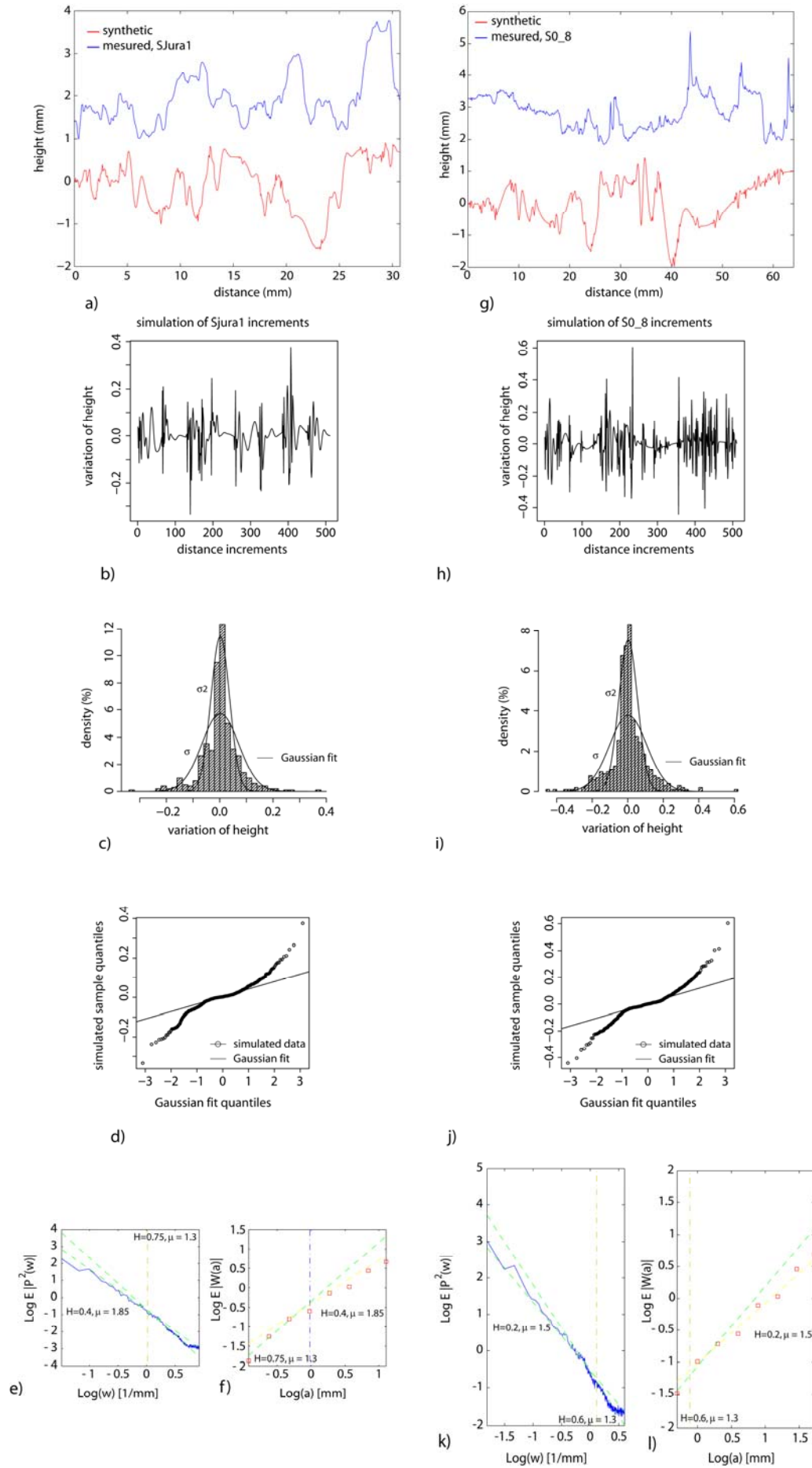
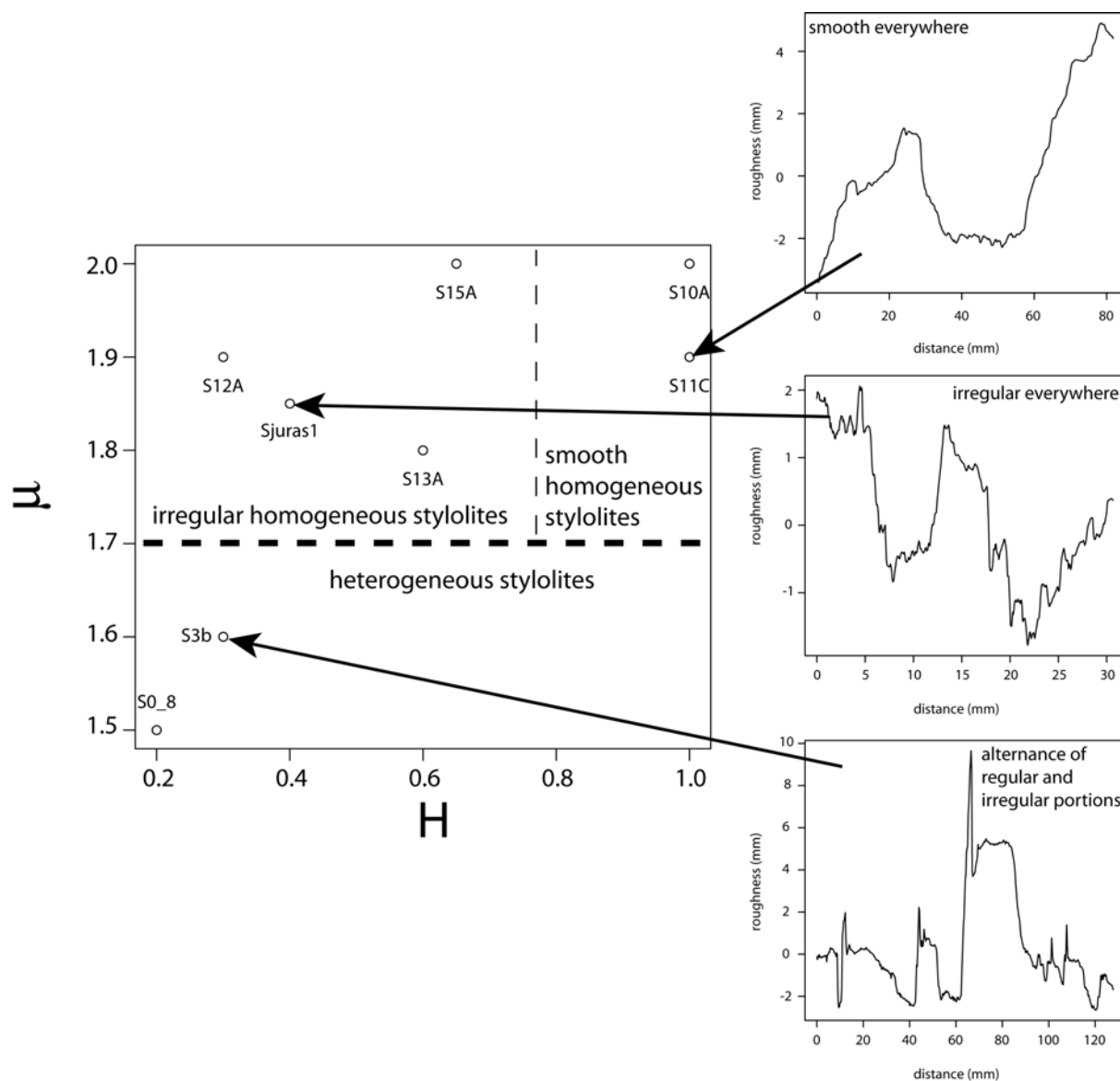


Figure 9. Using both values H and μ estimated at large length scale and at small length scale, one can reproduce different morphologies of stylolites using a combination of two SBPWS behaviors. a) Profile of the stylolite Sjura1 (see Table 1) and synthetic profile with the same parameters at small and large length scales as those estimated on Sjura1. b) Derivative of the synthetic signal of a) showing the increments. c) Histogram of the simulated increments. d) Quantile-quantile plot, as in figure 5 showing the departure from a Gaussian distribution. FPS (e) and AWC (f) spectra analysis for the synthetic signal having the same statistical properties as Sjura1. The green dashed straight lines at small and large length scales indicate the estimated slopes, showing the two characteristic slopes and the crossover length scale. g-l) Stylolite S0_8 and synthetic profiles with the same parameters as estimated on S0_8 and similar analysis than in a-d). FPS (g) and AWC (h) spectra of the synthetic stylolite showing the two characteristic slopes and the crossover length scale.

575



576
577
578
579
580
581

Figure 10. Various morphologies of stylolites based on their statistical properties at large length scale. Two main families can be identified, based on their statistical properties: those which are either regular or irregular everywhere, and those with alternating regular and irregular portions.

582 **Table 1.** Large and small length scale scaling exponents of the various stylolites.

stylolite	origin	H_{small}	μ_{small}	H_{large}	μ_{large}
Sjura1	Jura mountains	0.75	1.3	0.4	1.85
S12A	Vercors mountains	0.2	1	0.3	1.9
S11c	Burgundy mountains	0.7	1.35	1	1.9
S3b	Chartreuse mountains	0.5	1.4	0.3	1.6
S15A	Burgundy	0.6	1.4	0.65	2
S0_8	Jura mountains	0.6	1.3	0.2	1.5
S13A	Burgundy	0.9	1.8	0.55	1.8
S10A	Burgundy	0.85	1.4	1	2
Sdiss1	Experimental microstylolite	0.8	1.25	-	-
Sdiss2	Experimental microstylolite	0.75	1.2	-	-

583 1 For more details on the geological characteristics and composition of the stylolites, see Renard et al. (2004)
584 and Gratier et al. (2005) for the experimental microstylolites.